

Esophageal pressure as an estimate of average pleural pressure with lung or chest distortion in rats

Matteo Pecchiari¹, Stephen H. Loring², and Edgardo D'Angelo¹

¹Dipartimento di Fisiopatologia e dei Trapianti, Università di Milano, Milan, Italy, ²Department of Anesthesia and Critical Care, Boston, MA, USA;

Running title: P-V CURVES IN DISTORTION

DOI: 10.1016/j.resp.2013.02.006

Address correspondence to:
Edgardo D'Angelo
Dipartimento di Fisiopatologia e dei Trapianti
via Mangiagalli 32
20133 Milan, Italy
Tel. +39-02-50315440; Fax +39-02-50315430
E-mail edgardo.dangelo@unimi.it

Abstract

Pressure-volume curves of the lungs and chest wall require knowledge of an effective 'average' pleural pressure ($P_{pl_{av}}$), and are usually estimated using esophageal pressure as $P_{L_{es}}-V$ and $P_{W_{es}}-V$ curves. Such estimates could be misleading when P_{pl} becomes spatially non-uniform with lung lavage or shape distortion of the chest. We therefore measured $P_{L_{es}}-V$ and $P_{W_{es}}-V$ curves in conditions causing spatial non-uniformity of P_{pl} in rats. $P_{L_{es}}-V$ curves of normal lungs were unchanged by chest removal. Lung lavage depressed $P_{L_{es}}-V$ but not $P_{W_{es}}-V$ curves to lower volumes, and chest removal after lavage increased volumes at $P_L \geq 15$ cmH₂O by relieving distortion of the mechanically heterogeneous lungs. Chest wall distortion by ribcage compression or abdominal distension depressed $P_{W_{es}}-V$ curves and $P_{L_{es}}-V$ curves of normal lungs only at $P_L \geq 3$ cmH₂O. In conclusion, P_{es} reflects $P_{pl_{av}}$ with normal and mechanically heterogeneous lungs. With chest wall distortion and dependent deformation of the normal lung, changes of $P_{L_{es}}-V$ curves are qualitatively consistent with greater work of inflation.

keywords: abdominal distension, chest compression, chest wall mechanics, lung mechanics, rib cage restriction

1. Introduction

Pleural surface pressure (Ppl) is a clinically relevant parameter, the information it provides being useful in patient management during weaning (Jubran et al., 2005) and in the choice of positive end expiratory pressure (PEEP) in acute respiratory distress syndrome (ARDS) patients (Talmor et al., 2008). As direct measurements are impractical, esophageal pressure (Pes), usually obtained with the esophageal balloon technique, is commonly used to estimate Ppl in humans. Estimation of Ppl from Pes allows assessment of in situ transpulmonary ($P_{L_{es}}$) and transthoracic pressure ($P_{w_{es}}$) for determining lung and chest wall mechanics and respiratory muscle action.

There are practical concerns about the use of Pes in patients (de Chazal and Hubmayr, 2003) because of a variety of possible artifacts (Milic-Emili, 1984; Washko et al., 2006). Of greater concern is the fact that Ppl is not spatially uniform, as demonstrated by direct measurements in several animal species (Hoppin et al. 1969; D'Angelo et al., 1970, Agostoni and D'Angelo, 1974) and, indirectly, in humans (Milic-Emili et al., 1966). As a consequence, Ppl estimated by means of the esophageal balloon technique is customarily regarded as an effective 'average' pleural pressure, ($P_{pl_{av}}$), which is here defined as the spatially uniform pleural surface pressure that would be required to attain the observed lung volume and flow.

The use of Pes as an estimator of $P_{pl_{av}}$ has become a well accepted procedure in the presence of a normal respiratory system, and is justified by experiments in normal supine animals that show a) the transpulmonary pressure-volume curves measured using Pes ($P_{L_{es}}-V$) are similar to those measured in the excised lung (Wohl et al., 1968; Lay and Hildebrandt, 1978), and b) the average value of local elastic recoil pressures measured directly through pleural windows at functional residual capacity is similar to the transpulmonary pressure measured at the same volume after wide opening of the chest, irrespective of body position (D'Angelo et al., 1970). In humans, this conclusion has been indirectly supported by the observation that the shape of the $P_{L_{es}}-V$ curve is similar in different postures (Milic-Emili, 1984). Taken together, these findings suggest that in the presence of a normal respiratory system, Pes reflects $P_{pl_{av}}$.

In contrast, the use of Pes in pathological conditions has been questioned, because the degree of spatial non-uniformity of Ppl can increase markedly, and the more Ppl is non-uniform, the less likely Pes is to represent $P_{pl_{av}}$ (de Chazal and Hubmayr, 2003). Such non-uniformity could result from marked chest deformities or abdominal distension (Talmor et al., 2006; Behazin et al., 2010), or because of heterogeneous lung mechanical properties, as in ARDS (Maunder et al., 1986), moderate-to-severe COPD, cystic fibrosis, or pulmonary edema. If distortion is not marked, as is usual under physiological conditions, the ability of Pes to represent $P_{pl_{av}}$ can be evaluated by the

degree of similarity of the transpulmonary pressure-volume curves obtained before and after wide opening of the chest, as mentioned above. In the presence of marked lung isovolume distortion by the chest, this criterion may no longer be satisfied, because shape distortion by itself changes the lung's mechanical characteristics, making it less compliant. Thus, the transpulmonary pressure-volume curves obtained before and after opening of the chest would be expected to differ according to the degree to which the lung is distorted from its unconstrained shape.

In this study, we tested the ability of P_{es} to estimate $P_{pl_{av}}$ under conditions expected to cause marked spatial non-uniformity of lung mechanical properties or marked distortion due to an increased mismatch between intrinsic lung and chest wall shapes. Heterogeneity of regional mechanical properties reproducing an ARDS-like condition was obtained by repeated lung lavage. Lavage-induced heterogeneity should principally affect the lung and only marginally the chest wall, because the lung is more easily deformed, and lung-chest wall uncoupling with massive pneumothorax does not modify the relationship between transthoracic pressure and rib cage diameters in supine animals (D'Angelo et al., 1973). Moreover, no changes in the mechanical properties of the chest wall should occur with lung lavage. As a consequence, the volume-pressure curves of the relaxed chest wall obtained before and after surfactant depletion should be similar. This would support the use of P_{es} to estimate $P_{pl_{av}}$ even in the presence of marked spatial non-uniformity of lung mechanical properties and parenchymal distortion.

In addition, we have investigated the changes of the $P_{L_{es}}$ -V curve that occur with abdominal distension or rib cage compression causing marked shape distortion. Finally, to confirm our ability to reproduce results found in previous studies, we checked whether in normal rats the lung P-V curves recorded before and after widely opening the chest are superimposable.

2. Methods

Sixteen male Sprague-Dawley rats (weight range 390-480 g) were premedicated with diazepam ($10 \text{ mg}\cdot\text{kg}^{-1}$) and anesthetized with an intraperitoneal injection of pentobarbital sodium ($40 \text{ mg}\cdot\text{kg}^{-1}$) and chloral hydrate ($170 \text{ mg}\cdot\text{kg}^{-1}$). The animals were kept supine throughout the experiment. The trachea was cannulated, and polyethylene catheters were inserted into the jugular vein and carotid artery. A balloon-tipped catheter (inner diameter 0.6 mm) was placed in the lower third of the esophagus. The balloon was 20 mm long and 3 mm wide. In those animals in which abdominal distension was produced by inflating a 5 cm long rubber balloon advanced under the linea alba, a balloon similar to the esophageal one was placed between the diaphragm and the liver.

Airflow was measured with a heated Fleisch pneumotachograph no.0000 (HS Electronics, March-Hugstetten, Germany) and differential pressure transducer (Validyne MP45, ± 2 cmH₂O; Northridge, CA). The response of the pneumotachograph was linear over the experimental flow range. Pressures in the trachea (Ptr), esophagus, abdomen and systemic blood pressure were measured with pressure transducers (8507C-2 Endevco, San Juan Capistrano, CA; Statham P23Gb, Gould Electronics, Valley View, OH) connected to the side arm of the tracheal cannula, the esophageal and abdominal balloons, and carotid catheter, respectively. The appropriate positioning of the esophageal balloon was tested by measuring the ratio $\Delta P_{es} / \Delta P_{tr}$ during rapid, manual rib cage compressions with closed airways, similar to the occlusion test performed during spontaneous breathing (Baydur et al., 1982). There was no appreciable lag in the Pes signal or alteration in amplitude up to 20 Hz. The signals from the transducers were amplified (RS3800; Gould Electronics, Valley View, OH), sampled at 200 Hz by a 12-bit A/D converter (AT MIO 16E-10; National Instruments, Austin, TX), and stored on a desktop computer. Volume changes (ΔV) were obtained by numerical integration of the digitized airflow signal.

After completion of the surgical procedure, the rats were paralyzed with pancuronium bromide (1 mg·kg⁻¹) and ventilated with a specially designed, computer-controlled ventilator (D'Angelo et al., 2008), delivering water-saturated air from a high pressure source (4 atm) at constant flow, while Ringer-bicarbonate was continuously infused intravenously at a rate of 4 ml·kg⁻¹·h⁻¹, and epinephrine occasionally administered to maintain normal arterial blood pressure. Anesthesia and complete muscle relaxation were maintained with additional doses. Adequacy of anesthesia was judged from the absence of any sudden increase in heart rate and/or systemic blood pressure.

The pressure across the respiratory system, the transthoracic and in situ transpulmonary pressures were obtained as $P_{rs}=P_{tr}$, $P_{w_{es}}=P_{es}$, and $P_{L_{es}}=P_{tr}-P_{es}$, respectively, whereas P_L was used to indicate transpulmonary pressure in the presence of a spatially uniform P_{pl} , as it is the case with widely open chest, except for the small contact area in the lowermost part of the lung. Because measurements were performed in paralyzed animals under nearly static conditions (see below), these pressures essentially reflect the elastic properties of lung and chest wall.

2.1. Procedure and data analysis

Mechanical ventilation parameters included a tidal volume (V_T) of 8 ml·kg⁻¹, inspiratory time 0.25 s, expiratory time 0.5 s, and an end-inspiratory pause of 0.2 s. These ventilator settings

were maintained throughout the experiment. Flow was continuously integrated and displayed to monitor lung volume changes.

Three inflation P-V curves were obtained before (control) and during any given intervention by slowly inflating ($\sim 1 \text{ ml}\cdot\text{s}^{-1}$) the respiratory system from $\text{Ptr}=0$ to $\text{Ptr}=30 \text{ cmH}_2\text{O}$. Before each series of measurements the lungs were inflated 3-4 times to a Ptr of $\sim 26 \text{ cmH}_2\text{O}$ to ensure a uniform volume history. After each P-V curve, the lungs were allowed to deflate, and the expiratory valve was connected to a drum in which pressure was set to $-20 \text{ cmH}_2\text{O}$, the expired volume being the difference between the end-expiratory and minimal gas (or residual) volume (EELV-RV). Vital capacity (VC) was defined as sum of the inflation volume between Ptr 0 and $30 \text{ cmH}_2\text{O}$ and EELV-RV. Finally, the compliance of the respiratory system (C_{rs}), chest wall (C_w), and lung (C_L) were computed as the slope of each P-V curve in the volume range of the linear part of the control P-V curve.

In 9 rats, respiratory mechanics were assessed after the induction of acute lung injury by repeated intratracheal instillations and withdrawals of warm ($38 \text{ }^\circ\text{C}$) physiological saline, in aliquots of $30 \text{ ml}\cdot\text{kg}^{-1}$, until arterial oxygen tension fell below 80 mmHg . During the intervals between lavages and after lavage, the animals were ventilated with oxygen (90%) and a positive end-expiratory pressure (PEEP) of $6 \text{ cmH}_2\text{O}$.

In 7 rats, respiratory mechanics was assessed during rib cage compression with a rubber sheet and a Velcro band, which also provided moderate and marked restriction, respectively, or during abdominal distension obtained by inflating the abdominal balloon to increase subdiaphragmatic pressure to $\sim 7 \text{ cmH}_2\text{O}$ (moderate distension) and to $\sim 21 \text{ cmH}_2\text{O}$ (marked distension). Thereafter compression and distension were removed and respiratory mechanics reassessed.

The animals were killed with an overdose of anesthetic, and respiratory mechanics were measured again. The ventilator was disconnected, the silicon tube between the tracheal cannula and the pneumotachograph was clamped, and the thorax was quickly and widely opened, Ptr being continuously monitored. The increase of Ptr upon opening the chest (ΔPtr_{op}) was taken to represent $-\text{Ppl}_{av}$ at end-expiration with $\text{Ptr}=0 \text{ cmH}_2\text{O}$. It was also assumed that the difference between $-\Delta\text{Ptr}_{op}$ and Pes just before chest opening, which averaged $-0.3\pm 0.1 \text{ cmH}_2\text{O}$ (max $-1.1 \text{ cmH}_2\text{O}$), reflected artifacts like those described by Milic-Emili (1984) and Washko et al. (2006), and this difference was therefore added to the Pes measures obtained in the intact animal. The ventilator was connected to the pneumotachograph, and a PEEP equal to ΔPtr_{oc} was applied to the expiratory port of the ventilator to prevent the reduction of lung volume on clamp removal. Thereafter, respiratory mechanics were assessed as described above.

At the end of the experimental procedure, the lungs were removed, weighed immediately, and weighed again after desiccation overnight in an oven at 120 °C to calculate the wet-to-dry ratio (W/D). An estimate of the volume of saline remaining in the lungs was obtained by subtracting from the wet weight the product of the dry weight of these lungs and the mean W/D of normal lungs (4.23 ± 0.03) taken from a previous study (D'Angelo et al., 2008); this volume amounted to 1.1 ± 0.14 ml.

The animals were handled according to the guiding principles published by the National Institutes of Health and the study was approved by Ministero della Salute, Rome, Italy.

2.2. Statistics

Analyses were performed using SPSS 11.5 (SPSS Inc., Chicago, IL). Results are presented as mean \pm SE. Comparisons among experimental conditions were performed using the analysis of variance (ANOVA) for repeated measurements. When post-hoc tests were performed, a Bonferroni correction for multiple comparisons was applied. The level for statistical significance was taken at $P \leq 0.05$.

3. Results

3.1. Normal lung and chest wall mechanics

As shown in Fig. 1, the transpulmonary pressure-volume curves of 5 normal animals obtained before ($P_{L_{es}}-V$) and after wide opening of the chest wall (P_L-V) were superimposed almost completely, thus confirming that under normal conditions P_{es} adequately represents $P_{pl_{av}}$.

In the course of the experiments, a small downward convexity (hump) developed in untreated lungs at a transpulmonary pressure of ~ 17 cmH₂O (Fig. 1) that was not evident in the $P_{L_{es}}-V$ curves obtained soon after anesthesia and paralysis (Fig. 4, control). The presence of this hump, the nature of which is unknown (Zosky, 2008), will not be discussed further, being irrelevant to the present study.

3.2. Surfactant depleted lungs

Saline lavage shifted the inflation $P_{rs}-V$ and $P_{L_{es}}-V$ curves downward and to the right (Fig. 2), with the appearance of a marked knee (downward convexity) at a P_{rs} of ~ 15 cmH₂O and a $P_{L_{es}}$ of ~ 12 cmH₂O. Relative to control, the $P_{W_{es}}-V$ curve shifted downwards by ~ 1.8 ml, but its shape

was not affected by saline lavage. This shift mainly reflects the volume of saline that remained in the lungs at the time the P-V curves were obtained (33 ± 3 min after the completion of lung lavage). Indeed, the volume of saline left in the lungs averaged 2.05 ± 0.18 ml, while the excess lung water, estimated at the end of the experiment (104 ± 4 min after the completion of lung lavage), amounted to 1.1 ± 0.14 ml (see Methods); from these values and assuming a mono-exponential decay for saline absorption, the volume of saline left in the lungs at the time the post-lavage P-V curves should have been ~ 1.7 ml.

Relative to control conditions, EELV-RV and VC after bronchoalveolar lavage were decreased by $68\pm 5\%$ and $35\pm 4\%$, Crs and CL by $22\pm 7\%$, and $38\pm 8\%$, while Cw was unchanged.

Fig. 3 shows the effect of chest wall opening on the P-V curve of lavaged lungs. The response to lavage differed among the animals, and the PL_{es} -V curves were grouped post-hoc into two groups. The PL_{es} -V curves of the group with higher end-expiratory volume and PL_{es} (Group A) exhibited a greater slope both before and after the knee (Fig. 3). In both groups, the PL_{es} -V and PL-V curves were superimposed up to PL of ~ 15 cmH₂O. At higher pressures the curves diverged, with those obtained with a closed chest exhibiting progressively less volume with increasing transpulmonary pressure.

3.3. Chest wall distortion

Control values of VC and EELV-RV were 16.2 ± 0.7 and 2.8 ± 0.2 ml respectively; VC decreased by 25 ± 3 and $38\pm 4\%$ with the moderate and marked rib cage restriction, and by 21 ± 3 and $49\pm 5\%$ with the moderate and marked abdominal distension, respectively, while EELV-RV decreased by 57 ± 6 and $56\pm 9\%$ under the former and by 30 ± 6 and $31\pm 7\%$ under the latter conditions, respectively (Fig. 4).

The volume range in which the compliance of the respiratory system and its components was computed, extended from 6.1 ± 0.5 to 7.9 ± 0.5 ml. Control values of Crs, Cw, and CL were 0.80 ± 0.08 , 1.81 ± 0.29 and 1.58 ± 0.25 ml cmH₂O⁻¹ respectively; these values decreased by 37 ± 5 , 28 ± 9 , and $41\pm 10\%$, and by 59 ± 7 , 45 ± 12 , and $67\pm 4\%$ with moderate and marked rib cage restriction, respectively, by 38 ± 4 , 35 ± 10 , and $34\pm 12\%$, and by 67 ± 9 , 74 ± 6 , and $59\pm 12\%$ with moderate and marked abdominal distension, respectively.

Both ribcage compression and abdominal distension caused a rightward and downward shift of the Prs-V and Pw_{es}-V curve (Fig. 4). At EELV-RV, Pw_{es} increased by 3.2 ± 0.3 cmH₂O with both moderate and marked rib cage restriction, and by 1.6 ± 0.4 cmH₂O with both moderate and marked rib abdominal distension. Control and test PL_{es} -V curves superimposed up to PL_{es} and volumes of ~ 3

cmH₂O and ~30%VC, respectively. Thereafter, the test curves were progressively displaced downward toward the pressure axis (Fig. 4). On removal of both rib cage compression and abdominal distension, all parameters returned to control values.

4. Discussion

The principal results of this study in rats are *a)* P_{L_{es}}-V curves reflect the average pleural pressure in normal lungs (P_{pl_{av}}); *b)* P_{w_{es}}-V curves of the chest are not affected by lung lavage, indicating apparent validity of P_{es} estimates of P_{pl_{av}}; *c)* after saline lavage, changes in the lung P-V curves with wide chest opening are consistent with greater work required to expand the mechanically inhomogeneous lung when its shape is constrained by the chest wall; and *d)* marked distortion of chest wall stiffens both the P_{w_{es}}-V and P_{L_{es}}-V characteristic of the mechanically homogeneous lung, consistent with greater energy required for inflation with distortion.

4.1. Normal lung and chest wall mechanics

The P-V curves of normal lungs were not affected by widely opening the chest, suggesting that P_{es} reflects P_{pl_{av}}. In rats, the impact of the gravity dependent gradient of P_L should be minimal, and the weight of the heart and other thoracic content would not substantially increase P_{es} as it does in humans. The gravitational gradient has never been measured in supine rats. However, at the resting volume of the respiratory system (FRC), the top-to-bottom difference of P_L (Δ P_L) amounts to 2.5 cmH₂O in rats in the lateral posture (Agostoni and D'Angelo, 1971), while in rabbits the ratio of supine to lateral Δ P_L is 2.8/3.8=0.74 (D'Angelo et al., 1970). If this ratio applies also in rats, Δ P_L would be ~1.8 cmH₂O in the supine posture at FRC. The parenchymal distortion caused by this pressure difference apparently did not appreciably increase the elastic energy stored in the normal lung at any lung volume, because the curves obtained before (P_{L_{es}}-V) and after wide opening of the chest wall (P_L-V) were similar (Fig.1), in line with previous results in normal rats (Lay and Hildebrandt, 1978). This is the case with the greater Δ P_L that occurs at FRC in supine dogs (~4 cmH₂O; D'Angelo et al., 1970), because the P_{L_{es}}-V and the P_L-V curves are similar (Wohl et al., 1968), and, probably, also with the even greater Δ P_L (~6 cmH₂O; D'Angelo et al., 1970) of head-up dogs. Indeed, the P_L-V curves of a 30 cm high dog lung first suspended in air and then exposed to an artificial vertical gradient of 0.2 cmH₂O/cm were superimposed, apart from a small difference just above the inflationary inflection point (Glaister et al., 1973). However, marked differences in the P_L-V curves of dog lobes eventually occur when the heterogeneity of regional expansion and

dependent parenchymal distortion are further enhanced by the application of an hydrostatic gradient to the lung surface (Murphy et al., 1983). These findings confirm that under normal conditions, P_{es} provides an estimate of the effective average P_{pl} exerted on the lung surface, in spite of the remarkably non-uniform, gravity dependent distribution of P_{pl} and regional lung expansion.

4.2. Surfactant depleted lungs

Saline lavage caused changes in the $P_{L_{es}}-V$ curves characteristic of surfactant depletion (Fig 2). Inflation curves show effects of high surface tension and airspace closure more than expiratory curves. Surfactant removal and/or deactivation enhances regional heterogeneity with non-uniform alveolar expansion and increased amount of non-aerated tissue in dependent regions (Otto et al., 2008; Helm et al., 2009; Bickenbach et al., 2010), mimicking human ARDS (Caironi et al., 2010). Hence, mechanical heterogeneity and dependent distortion should have occurred in the lungs of our rats after surfactant depletion, thus increasing the spatial non-uniformity of P_{pl} and possibly preventing P_{es} from reflecting $P_{pl_{av}}$.

The comparison between the P-V curves of lavaged lungs obtained before ($P_{L_{es}}-V$) and after wide opening of the chest wall (P_L-V) shows that, in contrast with normal lungs, there is a divergence at higher lung volumes (Fig. 3). The possibility that this could indicate the inability of P_{es} to represent $P_{pl_{av}}$ acting on the apposed pleural surfaces is ruled out by the almost complete superimposition of the pre- and post-lavage $P_{w_{es}}-V$ curves, which can be accomplished by shifting the post-lavage $P_{w_{es}}-V$ curve upwards by ~ 1.8 ml, i.e. by the computed increase of extravascular water of lavaged lungs (see Results). There may also be changes of intrathoracic blood volume. A similar volume shift has been used to superimpose the volume-pressure curves of the chest wall obtained at FRC in supine dogs before and after oleic acid administration (Slutsky et al., 1980). As in the present experiments, this shift was attributed to an increase of extravascular lung water, the dimensions of the chest being unchanged and the volume of gas in the lung being markedly reduced. That no shift along the pressure axis was necessary to obtain an almost complete superimposition of the $P_{w_{es}}-V$ curves provides further support to the conclusion that even in the presence of marked, ARDS-like parenchymal heterogeneity, P_{es} represents a satisfactory approximation of $P_{pl_{av}}$. As a consequence, the difference between the $P_{L_{es}}-V$ and the P_L-V curves of lavaged lungs can be explained in terms of changes in the mechanical behavior of the lavaged lungs.

The most obvious effect of surfactant depletion by saline lavage is the fall in the resting volume of the respiratory system. On this basis, the animals were stratified into two groups

according to the level of end-expiratory volume and $P_{L_{es}}$ (Fig. 3). Relative to the $P_{L_{es}}$ -V curves of rats with higher FRC (Group A), those of rats with lower FRC (Group B) showed a much lower initial compliance, possibly due to a reduced number of open lung units, and a narrower range of pressures over which compliance increased during inflation, possibly indicating less widespread distribution of critical opening pressures. Furthermore, Group B rats exhibited a greater difference between the lung P-V curves obtained before and after chest opening. In both groups, the $P_{L_{es}}$ -V and PL-V curves were superimposed up to the pressure at divergence (Fig.3). As the anatomical dead space in these rats should amount to 0.4-0.5 ml (Olson, 1994), the initial part of the $P_{L_{es}}$ -V and PL-V curve should mainly reflect the mechanical properties of the airways (Group B) and of the airways plus some lung units (Group A). Above the pressure at divergence, the average slope of the PL-V curve became greater than that of the $P_{L_{es}}$ -V curve in both groups of animals. This is presumably due to differences in the pattern of recruitment of lung units caused by the non-uniform distribution of Ppl in the intact animal.

4.3. Chest wall distortion

Although superimposition of the $P_{L_{es}}$ -V and PL-V curves of normal lungs or of the $P_{w_{es}}$ -V curves of animals with normal and lavaged lungs supports the use of P_{es} as a valid estimate of $P_{pl_{av}}$, this may not always occur in the presence of a non-uniform distribution of local changes in Ppl due to marked chest wall shape distortion. If local Ppl values were to change uniformly with lung volume, the P-V curves with chest intact and open might differ by an amount independent of lung volume, thus keeping the same shape. In normal dogs, this is in fact the case during spontaneous breathing, whereas contrasting results have been obtained during passive inflation of the relaxed respiratory system (Hoppin et al., 1969; D'Angelo and Agostoni, 1973). Furthermore, non-uniform changes of local Ppl with passive inflation have been found in dogs with oleic acid-induced lung injury (Pelosi et al., 2001). Non-uniform changes in Ppl also occur in eviscerated rabbits, in which inflation causes an elongation of the lungs, with greater changes in cranio-caudal than transverse dimensions and smaller changes in Ppl on the diaphragmatic than costal surface and P_{es} (D'Angelo et al., 1999). Conversely, in rabbits with abdominal distension, lung inflation causes smaller changes of Ppl on the costal surface than on the diaphragmatic surface, consistent with greater changes in the lateral than cranio-caudal dimensions (D'Angelo et al., 2002). Furthermore, differences in tidal Ppl swings among various costal and diaphragmatic sites and between these sites and the esophagus have been observed in dogs with diaphragm paralysis or during maximal phrenic stimulation (D'Angelo et al., 1974). In normal seated subjects, esophageal pressure swings can

differ when measured at various levels as a result of different patterns of inspiratory muscles activation (D'Angelo, 1981; Irvin et al., 1984). These findings argue that care should be taken when interpreting P_{es} and the derived $P_{L_{es}}-V$ curves in the presence of markedly altered chest wall shape, the feature common to most of the conditions above.

Both rib cage compression and abdominal distension shifted the $P_{w_{es}}-V$ curve rightwards and downwards (Fig. 4), reflecting an increased stiffness that could be due to chest wall distortion with these interventions, besides direct contribution from the elastance of the chest binders. In order to make the $P_{L_{es}}-V$ curves more directly comparable, the rubber sheet and Velcro band, on the one hand, and two levels of abdominal distension, on the other hand, were applied to cause a similar decrease of the end-expiratory volume and increase in P_{es} . Hence, the $P_{L_{es}}-V$ curves obtained under all these conditions began from essentially the same point, superimposed at low lung volumes, but diverged from each other and from control, more so with stiffer chest or abdominal compartments (Fig. 4). Thus, marked changes of chest wall shape, necessarily transmitted to the lung, do not change P_{pl} distribution sufficiently to prevent P_{es} from reflecting $P_{pl_{av}}$ when the lung is at relatively low volumes and easily distortable (Lai-Fook et al., 1976). This may be not the case at higher volumes when the distortion affects a stiffer lung, because both criteria used to support P_{es} as a valid estimate of $P_{pl_{av}}$, namely superimposition of the $P_{L_{es}}-V$ and $P_{L}-V$ curves or of the $P_{w_{es}}-V$ curves, fail. Nevertheless, the rightward and downward shift of the $P_{L_{es}}-V$ with rib cage compression or abdominal distension is consistent with the increase of elastic energy stored at iso-volume because of lung distortion, and suggest that P_{es} might represent a qualitatively useful index of $P_{pl_{av}}$ even in the presence of marked changes in chest wall and lung shape.

4.4. Conclusion

In conclusion, the present study has shown that during muscle relaxation in rats, esophageal pressure reliably reflects the average pressure acting on the surface of the lung both under normal conditions and in the presence of lung distortion due to non-homogeneity of lung mechanical properties. When lung distortion is the consequence of chest wall distortion, lung and chest wall $P-V$ curves shift downwards, qualitatively in line with the additional elastic work required for inflation with distortion. It seems reasonable to believe that these conclusions also apply to esophageal pressure measurements in humans under both normal and pathological conditions, although no direct evidence is available.

References

- Agostoni, E., D'Angelo, E., 1971. Comparative feature of the transpulmonary pressure. *Respir. Physiol.* 11: 76-83.
- Baydur, A, Behrakis, P.K., Zin, W.A., Jaeger, M., Milic-Emili, J., 1982. A simple method for assessing the validity of the esophageal balloon technique. *Am. Rev. Respir. Dis.* 126:788-791.
- Behazin, N, Jones, S.B., Cohen, R.I., Loring, S.H., 2010. Respiratory restriction and elevated pleural and esophageal pressures in morbid obesity. *J. Appl. Physiol.* 108:212-218.
- Bickenbach, J., Czaplik, M., Dembiski, R., Pelosi, P., Schroeder, W., Marx, G., Rossaint, R., 2010. In vivo microscopy in a porcine model of acute lung injury. *Respir. Physiol. Neurobiol.* 172: 192-200.
- Caironi, P., Cressoni, M., Chiumello, D., Ranieri, M., Quintel, M., Russo, S.G., Cornejo, R., Bugeo, G., Carlesso, E., Russo, R., Caspani, L., Gattinoni, L., 2010. Lung opening and closing during ventilation of acute respiratory distress syndrome. *Am. J. Respir. Crit. Care Med.* 181: 578-586.
- D'Angelo, E., 1981. Cranio-caudal rib cage distortion with increasing inspiratory airflow in man. *Respir. Physiol.* 44: 215-237.
- D'Angelo, E., Agostoni, E., 1973. Continuous recording of pleural surface pressure at various sites. *Respir. Physiol.* 19: 356-368.
- D'Angelo, E., Bonanni, M.V., Michelini, S., Agostoni, E., 1970. Topography of the pleural surface pressure in rabbits and dogs. *Respir. Physiol.* 8: 204-229.
- D'Angelo, E., Giglio, R., Lafontaine, E., Bellemare, F., 1999. Influence of abdomen on respiratory mechanics in supine rabbits. *Respir. Physiol.* 115: 287-299.
- D'Angelo, E., Koutsoukou, A., Della Valle, P., Gentile, G., Pecchiari, M., 2008. Cytokine release, small airway injury, and parenchymal damage during mechanical ventilation in normal open-chest rats. *J. Appl. Physiol.* 104: 41-49.
- D'Angelo, E., Michelini, S., Miserocchi, G., 1973. Local motion of the chest wall during passive and active expansion. *Respir. Physiol.* 19: 47-59.
- D'Angelo, E., Pecchiari, M., Acocella, F., Monaco, A., Bellemare, F., 2002. Effects of abdominal inflation on breathing pattern and respiratory mechanics in rabbits. *Respir. Physiol.* 130: 293-304.
- D'Angelo, E., Sant'Ambrogio, G., Agostoni, E., 1974. Effect of diaphragm activity or paralysis on distribution of pleural pressure. *J. Appl. Physiol.* 37: 311-315.

- de Chazal, I., Hubmayr, R.D., 2003. Novel aspects of pulmonary mechanics in intensive care. *Brit. J. Anaesth.* 91: 81-91.
- Glaister, D.H., Schroter, R.C., Sudlow, M.F., Milic-Emili, J., 1973. Bulk elastic properties of excised lungs and the effect of a transpulmonary pressure gradient. *Respir. Physiol.* 17: 347-364.
- Helm, E., Talakoub, O., Grasso, F., Engelberts, D., Alirezaie, J., Kavanagh, B.P., Babyn, P., 2009. Use of dynamic CT in acute respiratory distress syndrome (ARDS) with comparison of positive and negative pressure ventilation. *Eur. Radiol.* 19: 50–57.
- Hoppin, F.G., Jr., Green, I.D., Mead, J., 1969. Distribution of pleural surface pressure in dogs. *J. Appl. Physiol.* 27: 863-873.
- Irvin, C.G., Sampson, M., Engel, L., Grassino, A.E., 1984. Effect of breathing pattern on esophageal pressure gradients in humans. *J. Appl. Physiol.* 57: 168-175.
- Lai, Y., Hildebrandt, L., 1978. Respiratory mechanics in the anesthetized rat. *J. Appl. Physiol.* 45: 255-260.
- Lai-Fook, S.J., Wilson, T.A., Hyatt, R.E., Rodarte, J.R., 1976. Elastic constants of inflated lobes of dogs lungs. *J. Appl. Physiol.* 40: 508-513.
- Jubran, A., Grant, B.J.B., Laghi, F., Parthasarathy, S., Tobin, M.J., 2005. Weaning prediction: esophageal pressure monitoring complements readiness testing. *Am. J. Respir. Crit. Care Med.* 171: 1252-1259.
- Maunder, R.J., Shuman, W.P., Mc Hugh, J.W., Marglin, S.I., Butler, J., 1986. Preservation of normal lung regions in the adult respiratory distress syndrome: analysis by computed tomography. *J.A.M.A.* 255: 2463-2465.
- Milic-Emili, J., Henderson, J.A., Dolovich, M.B., Trop, D., Kaneko, K., 1966. Regional distribution of inspired gas in the lung. *J. Appl. Physiol.* 21: 749-759.
- Milic-Emili, J., 1984. Measurement of pressures in respiratory physiology. In: *Techniques in the life sciences*. Shannon, Ireland: Elsevier Scientific, pp. 1–22.
- Murphy, B.G., Plante, F., Engel, L.A., 1983. Effect of a hydrostatic pleural pressure gradient on mechanical behavior of lung lobes. *J. Appl. Physiol.* 55: 453-461.
- Olson, E.B., Jr., 1994. Physiological dead space increases during initial hours of chronic hypoxemia with or without hypocapnia. *J. Appl. Physiol.* 77: 1526-1531.
- Otto, C.M., Markstaller, K., Kajiakawa, O., Karmrodt, J., Syring, R.S., Pfeiffer, B., Good, V.P., Frevert, C.W., Baumgardner, J.E., 2008. Spatial and temporal heterogeneity of ventilator-associated lung injury after surfactant depletion. *J. Appl. Physiol.* 104: 1485-1494.

- Pelosi, P., Goldner, M., McKibben, A., Adams, A., Eccher, G., Caironi, P., Losappio, S., Gattinoni, L., Marini, J.J., 2001. Recruitment and derecruitment during acute respiratory failure. *Am. J. Respir. Crit. Care Med.* 164: 122-130.
- Slutsky, A.S., Scharf, S.M., Brown, R., Ingram, R.H., 1980. The effect of oleic acid-induced pulmonary edema on pulmonary and chest wall mechanics in dogs. *Am. Rev. Respir. Dis.* 121: 91-96.
- Talmor, D., Sarge, T., O'Donnel, C.R., Mahotra, A., Lisbon, A., Loring, S.H., 2006. Esophageal and transpulmonary pressure in acute respiratory failure. *Crit. Care Med.* 34: 1389-1394.
- Talmor, D., Sarge, T., Mahotra, A., O'Donnel, C.R., Ritz, R., Lisbon, A., Novack, V., Loring, S.H., 2008. Mechanical ventilation guided by esophageal pressure in acute lung injury. *N. Engl. J. Med.* 359: 2095-2104.
- Washko, G.R., O'Donnell, C.R., Loring, S.H., 2006. Volume-related and volume-independent effects of posture on esophageal and transpulmonary pressures in healthy subjects. *J. Appl. Physiol.* 100: 753-758.
- Wohl, M.E.B., Turner, J., Mead, J., 1968. Static volume-pressure curves of dog lungs-in vivo and in vitro. *J. Appl. Physiol.* 24: 348-354.
- Zosky, G.R., Janosi, T.Z., Adamicza, A., Bozanich, E.M., Cannizzaro, V., Larcombe, A.N., Turner, D.J., Sly, P., Hantos, Z., 2008. The bimodal quasi-static and dynamic elastance of the murine lung. *J. Appl. Physiol.* 105:685-692.

Legends

Fig. 1. Inflation transpulmonary pressure-volume curves obtained with closed ($P_{L_{es}}-V$) and widely open chest (P_L-V) in 7 anesthetized, paralyzed, supine rats with normal lungs. Bars are SE.

Fig. 2. Inflation pressure-volume curves of the respiratory system ($P_{rs}-V$), chest wall ($P_{w_{es}}-V$), and lungs ($P_{L_{es}}-V$) in 9 anesthetized, paralyzed supine rats before (control) and after bronchoalveolar (BA) lavage. Bars are SE.

Fig. 3. Inflation transpulmonary pressure-volume curves with closed ($P_{L_{es}}-V$) and open chest (P_L-V) in 9 anesthetized, paralyzed supine rats after bronchoalveolar lavage. The animals were stratified post-hoc into Groups A and B according to the level of end-expiratory volume and $P_{L_{es}}$. Bars are SE.

Fig. 4. Inflation pressure-volume curves of the respiratory system ($P_{rs}-V$), chest wall ($P_{w_{es}}-V$), and lungs ($P_{L_{es}}-V$) in 7 anesthetized, paralyzed, supine normal rats before (control) and during rib cage compression with moderate or marked restriction (upper panels), and during moderate or marked abdominal distension (lower panels). The volume range in which compliance was computed under each condition is indicated by the dotted lines. Bars are SE.

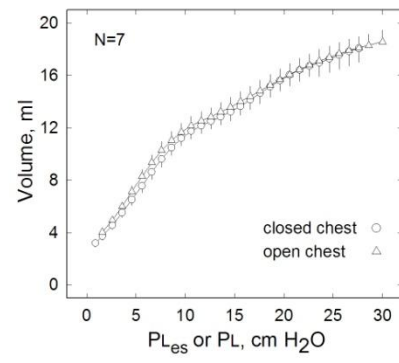


Figure 1

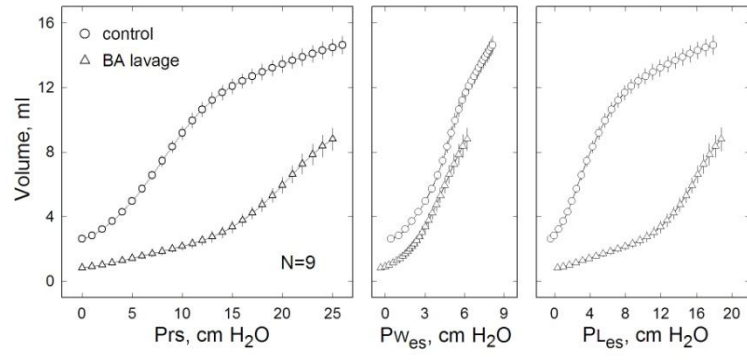


Figure 2

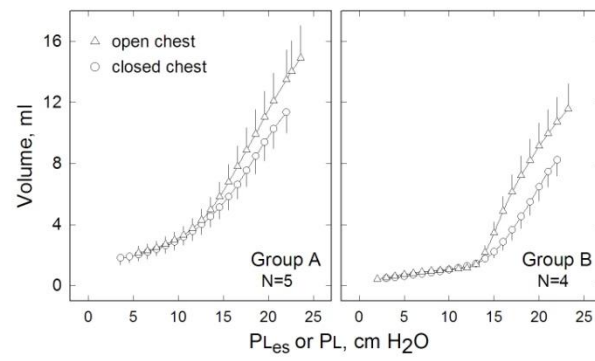


Figure 3

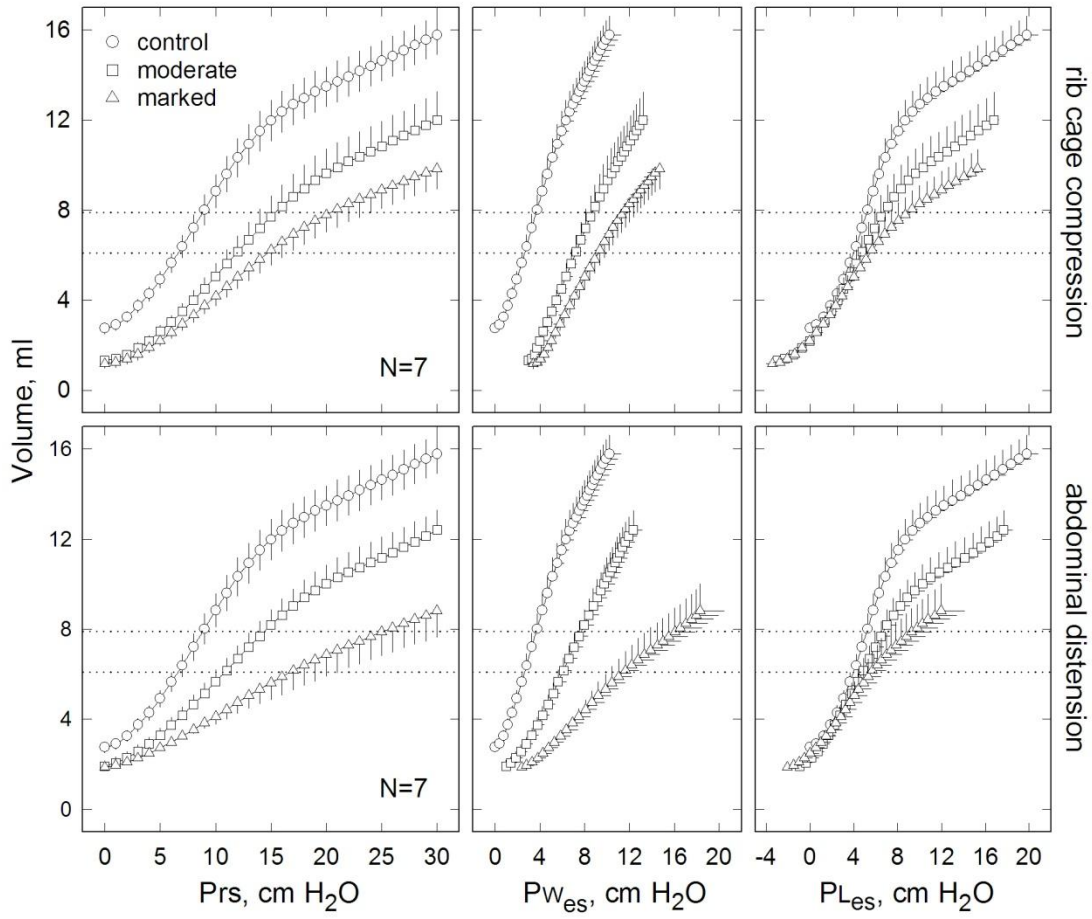


Figure 4